Chemistry Europe
European Chemical Societies Publishing

WILEY VCH

Excellence in Chemistry Research

Announcing our new flagship journal

- Gold Open Access
- Publishing charges waived
- Preprints welcome
- Edited by active scientists

Meet the Editors of *ChemistryEurope*

Luisa De Cola
Università degli Studi di Milano Statale, Italy

Ive Hermans
University of Wisconsin-Madison, USA

Ken Tanaka
Tokyo Institute of Technology, Japan

ChemSusChem

Research Article
doi.org/10.1002/cssc.202202196

Chemistry Europe
European Chemical Societies Publishing

www.chemsuschem.org

Life Cycle Impact Assessment of Solution Combustion Synthesis of Titanium Dioxide Nanoparticles and Its Comparison with More Conventional Strategies

Roberto Rosa,*[a] Enrico Paradisi,[b] Magdalena Lassinantti Gualtieri,[b] Consuelo Mugoni,[b] Grazia Maria Cappucci,[a] Chiara Ruini,[a] Paolo Neri,[a] and Anna Maria Ferrari[a]

This paper represents the first attempt to quantitatively and reliably assess the environmental sustainability of solution combustion synthesis (SCS) with respect to other soft chemistry strategies, which are more conventionally employed in the preparation of engineered oxide nanomaterials, namely hydrolytic and non-hydrolytic sol–gel syntheses (i.e., HSGS and NHSGS). Indeed, although SCS is well known to rely on significant reduction in the energy as well as time required for the obtainment of the desired nanocrystals, its quantitative environmental assessment and a detailed comparison with other existing synthetic pathways represents an absolute novelty of high scientific desirability in order to pursue a more sustainable development in the inorganic chemistry as well as materials science research fields. TiO_2 nanoparticles were selected as the material of choice, for the production of which three slightly modified literature procedures were experimentally reproduced and environmentally evaluated by the application of the comprehensive life cycle assessment (LCA) methodology. Particularly, SCS was compared from an environmental perspective with sol–gel approaches performed both in water and in benzyl alcohol. The results of the present study were also framed among those recently obtained in a systematic study assessing seven further chemical, physical, and biological routes for the synthesis of TiO_2 nanoparticles, comprising also flame spray pyrolysis (typically used in industrial productions), highlighting and quantifying the excellent environmental performances of SCS.

Introduction

In the evaluation and selection of a synthetic strategy for the preparation of a desired chemical compound, conventional parameters like yield, reaction time and cost of the precursors needed, are those on which the choice is typically based. Moreover, further considerations on the size and shape of the desired nanocrystals are required in the synthesis of inorganic engineered nanomaterials,[1] since these aspects are of paramount importance for the displaying of the quantum size effect, thus, for the plenty of their exciting possible applications.[2,3] With the diffusion of sustainable practices in chemistry and engineering fields of study,[4–6] the so-called green metrics[7,8] started covering a significant role, even if mainly limited to organic chemistry. However, by bearing in mind the significant lack of information on long-term environmental as well as human health impacts of nanomaterials, the existence of trustworthy green metrics parameters also for the different preparation strategies of these inorganic materials appears of great importance, to pursue a more sustainable development. Indeed, the production of nanoparticles was recognized as more environmentally impacting with respect to other bulk chemicals,[9] with the production phase being the largest contribution to the environmental impact of their life cycle.[10]

Among the existing soft chemistry strategies, that allow a subtle control over the phase, the size and the shape of engineered nanomaterials, solution combustion synthesis (SCS)[11] is considered one of the most attractive, due to its low amounts of energy and time required.[11,12] Indeed, SCS exploits exothermic self-sustaining reactions occurring typically in aqueous solutions containing a mixture of an oxidizer (e.g., a metal nitrate) and an organic fuel among which urea, thiourea, citric acid and glycine are the most widely employed. After homogeneously mixing the reactants, the resulting solution is concentrated to obtain a viscous medium which is subsequently ignited, the latter being the only energy requirement from the surrounding environment, due to the high amount of heat released by the combustion reaction itself. As a result of its exothermic character, the reaction ignited is typically completed in seconds and the high temperatures attained ($\approx$1500 °C) promote the crystallization of the nanomaterials obtained, so that additional calcinations treatments are typically unnecessary.

Although originally developed for the preparation of oxides, SCS has nowadays reached a high level of controllability and

[a] Prof. Dr. R. Rosa, G. M. Cappucci, C. Ruini, P. Neri, Prof. Dr. A. M. Ferrari
Department of Sciences and Methods for Engineering
University of Modena and Reggio Emilia
via G. Amendola 2, 42122 Reggio Emilia (Italy)
E-mail: roberto.rosa@unimore.it
[b] Dr. E. Paradisi, Dr. M. Lassinantti Gualtieri, Dr. C. Mugoni
Department of Engineering "Enzo Ferrari"
University of Modena and Reggio Emilia
via P. Vivarelli 10, 41125 Modena (Italy)

Supporting information for this article is available on the WWW under https://doi.org/10.1002/cssc.202202196

versatility,[13] allowing synthesizing different nanosized compounds like sulfides,[14–16] metals and alloys,[17–20] by playing on the fuel selected as well as on the fuel to oxidizer ratio. Furthermore, SCS up scaling possibility was demonstrated by exploiting a continuous process able to reach a nanoparticles productivity of 0.5–2 kg h^{-1}.[21,22]

Although several researchers[12,13,23] recognized SCS as a sustainable strategy of synthesis, mainly due to the low amounts of necessary energy and time, there is still a need for a reliable, accurate and quantitative environmental assessment.

In this study we have performed a comparison between SCS and routinely employed synthetic pathways such as hydrolytic sol–gel synthesis (HSGS) and non-hydrolytic sol–gel synthesis (NHSGS), by applying the life cycle assessment (LCA) methodology. The latter consists in a modeling framework to assess resource use, emissions, and related environmental impacts throughout the life cycle of a given product, process, service or system.[24]

TiO_2 nanoparticles have been identified as the ideal candidate material for this study, since it represents one of the most studied and applied semiconductors and photocatalysts, owing to its unique physicochemical properties.[25,26] Moreover, several TiO_2 nanoparticle syntheses have been evaluated by employing the LCA methodology,[27–29] including also a study performed by some of the present authors,[30] devoted to the environmental sustainability assessment of the hydrolytic sol–gel synthesis of titania nanoparticles, according to a patented procedure.[31] In that study, the environmental impact of the batch production of a 6 wt% TiO_2 nanoparticles suspension, was mainly caused by the energy consumptions needed for mixing and heating the reaction mixture, followed by the contributions deriving from the use of titanium(IV) isopropoxide precursor.[30] The Altair hydrochloride process[32] for the production of TiO_2 nanoparticles was instead assessed by Grubb and Bakshi,[27] who highlighted the major contributions of ilmenite mining and the steam generation for most of the impact categories considered.

Synthetic approaches for the continuous flow production of titania nanoparticles were evaluated from an environmental perspective by Caramazana-Gonzalez et al.[28] and by Tsang et al.[29] Particularly, different titanium precursors and different reaction conditions (i.e., solvothermal and hydrothermal ones) were evaluated in the first work,[28] and it was found that the hydrothermal synthesis employing titanium oxysulphate precursor resulted in the lowest values of global warming potential ($< 12\ kg_{CO_2\ equiv.}\ kg^{-1}$ TiO_2 nanoparticles) and cumulative energy demand ($< 149\ MJ\ kg^{-1}$ TiO_2 nanoparticles). Supercritical fluid (i.e., water + ethanol) flow synthesis of TiO_2 nanoparticles was shown to possess lower environmental impacts with respect to a conventional precipitation approach, independently of the impact category considered in the study by Tsang et al.,[29] with a 30% reduction in cumulative energy demand and a 55% reduction in climate change potential.

The main limitation of such studies was the lack of consistency with respect to the scope definition, functional unit and impact assessment method considered during the LCA analyses, thus making the comparison of the environmental performances among different synthetic routes not possible at all. On the opposite, very recently Wu et al.[33] performed a systematic study aimed at comparing from an environmental perspective seven different synthetic strategies for titania nanoparticles, including chemical, biological and physical routes, the latter comprising also flame spray pyrolysis, that represents the technology adopted by Degussa to produce the standard P25 TiO_2 photocatalyst.[34]

In that systematic study, for the first time different TiO_2 nanoparticles synthesis methods were compared not only on the basis of the amount of product, but also by accounting for its quality, in terms of specific surface area, crystallinity and photocatalytic activity. Independent of the functional unit considered (i.e., mass based, surface area based or photocatalytic activity based) the chemical methods resulted significantly less environmental impacting with respect to physical approaches, mainly due to the higher amounts of gases and electricity required by the latter ones. The bacterial culture media, and the low degree of development and optimization were mainly responsible for the high environmental burdens associated to biosynthesis.

Although systematically conducted, the work by Wu et al.[33] assessed published procedures without experimentally replicating them, thus it necessarily neglected potentially fundamental contributions, like for example the reaction waste and the amounts of solvents used for the reaction workup. Further contributions which were not included in the systematic study include emissions of chemicals and transport ones.

On the opposite the present work is devoted to the environmental sustainability assessment of SCS, HSGS and NHSGS procedures, that were experimentally replicated in the laboratory, in order to account also for the above-mentioned contributions which are typically neglected. Therefore, in pursuing the natural continuation of our previous research,[30] and in order to add further very promising synthetic techniques to those environmentally assessed and to make them comparable on a reliable basis with those recently evaluated by LCA methodology,[33] this manuscript represents a step nearer to the establishment of environmental rankings comprising the majority of the existing preparation procedures of a desired nanomaterial, provided with reliable and quantitative data which will be easily accessible by inorganic chemists and materials scientists worldwide. These data could potentially act as guidelines for the responsible production of engineered oxide nanomaterials, thus, partially contributing to the pursuing of at least number twelve of the United Nations Sustainable Development Goals (UN-SDGs).[35] Indeed, in order for nanotechnology to effectively enable sustainability, some research outcomes in the field have been identified as highly needed, including the use of sustainability metrics in the synthesis of nanomaterials of any kind and at any scale, as well as the overall energy balance of their life cycle.[36]

Life cycle assessment

The LCA methodology was applied according to the ISO 14040[37] and 14044:[38] its constituting phases are detailed hereafter.

Goal and scope definition

Goal definition

The goal of this study was to quantify, "from cradle to gate" (i.e., from raw materials extraction to manufacture) the environmental impacts of SCS of TiO_2 nanoparticles and to compare them with those associated to more conventionally employed hydrolytic and non-hydrolytic sol–gel syntheses, the first one assisted by HCl and the second one employing the benzyl alcohol route (BAR). A further goal was to reliably compare the three assessed chemical strategies with further TiO_2 synthetic strategies assessed in the systematic study performed by Wu et al.[33] (i.e., sol–gel, hydrothermal, solvothermal, microemulsion, flame spray pyrolysis, radio frequency thermal plasma and a biological route).

System, functional unit, and function of the system

The system object of the present study is the synthesis of TiO_2 nanoparticles (NPs) performed by SCS as well as by HSGS and NHSGS.

Similar to the systematic study performed by Wu et al.,[33] one kilogram of TiO_2 NPs was selected as the initial functional unit. The yield of the synthesis considered was accounted for, by considering the mass of the as-isolated powders, their crystallinity degree (as determined by XRD analysis) and their humidity degree (as determined before the BET analysis).

Since the function of the system object of the present study is various, including the high absorption capacity as well as the photocatalytic activity that are dominated by the surface area, size and crystallinity, a further comparative assessment among the synthetic procedures, was performed by considering a surface area-based functional unit, as also proposed in further works.[33,39] At this purpose, the environmental impacts were re-scaled in order to refer them to 1000 m^2 of surface area. Moreover, to reduce the number of independent variables in comparing the different synthetic strategies, standard P25 Degussa TiO_2 nanoparticles, synthesised by flame spray pyrolysis[34] and consisting in a 3:1 of anatase to rutile ratio,[40] was used as reference. In doing so, an additional energy contribution (necessary to obtain the desired 3:1 ratio) was considered in the three assessed synthetic strategies as also performed by Wu et al.[33]

The system boundaries considered for the assessment of the three synthetic approaches range from the cradle to the gate, thus neglecting their use as well as their end of life. They are summarised in the flowcharts reported in Figures S1–S3 of the Supporting Information.

Life cycle inventory (LCI) and life cycle impact assessment (LCIA)

The data employed for the LCI phase were directly collected in the laboratory during replication of the synthetic procedures selected. Replication of the procedures allowed to account in the LCA for the energies effectively involved, the equipment used, as well as the waste generated during synthesis and work-up steps. For the electric energy consumptions, the power of the equipment employed and their time of usage were considered, similarly to other works devoted to the assessment of lab-scale procedures.[39,41]

The inventories of the equipment used are detailed in Tables S1–S13, together with the considerations and assumptions made for their modelling.

The possible emissions into the atmosphere were also included in the present study. At this latter regard, instead of basic process calculations, advanced process calculations[42] were performed to account for emissions of at least the liquid chemicals employed. Particularly, the working losses, L_W,[43] thus those related to handling of chemicals, were adapted, and considered in the present study. The details for the calculation of L_W used in this study are reported in Equation (1), where V is the volume of the chemical employed [L], V_m is the molar volume [L] the unit was modified to match journal style, of ideal gas at 0 °C and 1 atm, T is the average ambient temperature [K], P_i^{sat} is the vapour pressure of liquid [mmHg], MW is the molecular weight of chemical [g mol^{-1}], K_N is the turnover factor (dimensionless) and K_P is the working loss product factor (dimensionless). The value of K_N is dependent on the number of turnovers N [yr^{-1}] of the chemical tank as defined by Equation (2), where V_t is the tank capacity.[43] Particularly, when $N > 36$, K_N is given by Equation (3), while $K_N = 1$ for $N \leq 36$. Due to the lab scale character of this study, thus to the small volumes of chemicals employed, K_N was considered equal to 1. By definition,[43] K_P is equal to 1 for all the organic liquids, except for crude oil for which it assumes the value of 0.75. Therefore, in this study K_P was considered equal to 1.

$$L_W = \frac{V}{V_m}\left(\frac{273.15}{T}\right)\left(\frac{P_i^{sat}}{760}\right)(MW)K_N K_P \quad (1)$$

$$N = \frac{V}{V_t} \quad (2)$$

$$K_N = \frac{(180 + N)}{6N} \quad (3)$$

The 99% of each emitted substance was considered to be retained by an aspiration system endowed with an activated carbon filter.[44] The inventories of the aspiration system and the filter are detailed in Tables S14 and S15, respectively.

It is worthy to be reminded that the above-mentioned emission calculations would need to be re-considered in the up-scaling of the assessed syntheses to industrial processes.

The potential release of nanoparticles, together with the potentially associated nanospecific impacts, were not considered in this study.

The environmental impact contribution of the transport of materials and equipment was also considered. In doing so, 100 km was assumed as a reasonable average distance.[44,45] Particularly, the road freight transportation by diesel EURO 6 (i.e., meeting the six and the last European Union emissions standard)[46] lorries, with two lorry capacities, i.e., 3.5–7.5 and 16–32 metric tons were considered.[44,45]

The modelling of the processes was done by employing datasets of the Ecoinvent database (EID, version 3.8).[47,48] Particularly, an attributional approach was followed,[47] thus the "Allocation at the point of substitution" (i.e., APOS) system model was employed. The precise datasets employed are detailed in the inventory tables in the Supporting Information.

To make our results comparable with those obtained in the systematic study performed by Wu et al.,[33] their same inventories were considered in modelling of electricity mix and titanium(IV) isopropoxide precursor (Tables S16 and S17). The electricity mix used and detailed in Table S16 considers the U.S. electricity generated by each fuel source in 2017.[33]

For their modelling, the U.S. Life Cycle Inventory Database (USLCI)[49] was also employed.

The inventories of the modelled SCS, HSGS and NHSGS are detailed in Tables S18–S20.

The inventories were modelled in SimaPro 9.3.0.2.[50] The LCIA was performed by using the global scale-oriented ReCiPe2016 method both at midpoint and endpoint levels, with a hierarchist (H) perspective and average weighting set (A).[51] The selected impact assessment method is one of the most widely accepted and scientifically applied global methods,[52,53] since it accounts for a significantly higher number of impact categories with respect to other methods.[54]

However, to frame the impacts of SCS, HSGS and NHSGS within the results obtained in the systematic study by Wu et al.,[33] our inventories were re-adjusted. Particularly, they were modified in terms of some of the energy contributions, since that systematic study[33] was performed on not-replicated procedures. Thus, the energy requirements for heating and drying were calculated according to Equations (4) and (5) respectively, where m is the mass [kg] of the compound to be heated, C_p is its heat capacity [kJ kg^{-1} K^{-1}], ΔT the temperature difference [K] between its temperature and the environment, and H_v is its heat of vaporization [kJ kg^{-1}]. More importantly, the contributions of transport, equipment, emissions and waste treatment were completely neglected in the systematic study, thus they were also eliminated in the adjusted inventories for SCS, HSGS and NHSGS, which are reported in Tables S21–S23.

$$Q_{heating} = mC_p\Delta T \quad (4)$$

$$Q_{drying} = \sum mH_V \quad (5)$$

For this latter comparison, the LCIA was performed by the midpoint-oriented TRACI 2.1 method,[55] as performed in the work by Wu et al.[33]

Results and Discussion

Characterization of the synthesized TiO_2 nanoparticles

The physicochemical characteristics of the TiO_2 nanoparticles synthesized by SCS, HSGS and NHSGS are summarized in Table 1. The results slightly differ from those reported in the works of reference, highlighting the importance of experimentally reproducing the published procedures before performing any environmental assessment. The Rietveld refinement outputs for the three synthesis methods are reported in Figures S4–S6, whereas galleries of bright-field TEM images collected from the nanopowders are shown in Figures S7–S9. The particle size determined from manual processing of TEM images possibly corresponds to the crystallographic coherent length as a good agreement is found with XRPD data (see Table 1).

As visible from Table 1 the three synthetic procedures led to different crystalline polymorphs percentages, thus to different materials not necessarily interchangeable in their final application.[56] This is, indeed, the main reason why two different functional units (i.e., 1 kg and 1000 m^2 surface area) were selected in this study and why an additional energy contribution was considered for all the three syntheses to reach a 3:1 anatase-to-rutile ratio.

Environmental impacts of SCS, HSGS and NHSGS

The environmental impacts of the three assessed synthetic strategies, are detailed at a midpoint level in Tables 2 and 3, for 1 kg and 1000 m^2 functional units respectively. The relative impacts among the three syntheses are depicted in Figure 1.

Independent of the functional unit considered, the environmental impacts follow the general trend: SCS < HSGS < NHSGS.

By considering the mass-based functional unit (Figure 1a), SCS possesses the lower environmental impact with respect to HSGS and NHSGS for all the impact categories considered, except for SOD (stratospheric ozone depletion, $kg_{CFC\text{-}11equiv.}$). SCS has a higher SOD than HSGS.

Table 1. Summary of physicochemical characteristics of the TiO_2 nanoparticles synthesized by SCS, HSGS and NHSGS strategies. The isotropic size of coherently diffracting domains determined by XRPD are reported together with the size determined by TEM.

Synthetic procedure	Phase [wt%] anatase	rutile	brookite	amorphous	Crystallite size [nm] anatase/rutile/brookite	Particle size [nm]	Humidity [%]	BET SSA [m^2 g^{-1}]
SCS	87.0±0.7	1.6±0.1	–	11.4±0.7	9.9±0.1/172±42/–	7±3	5.76	130.6
HSGS	54.7±0.6	–	40.9±0.6	4.4±0.8	4.6±0.1/–/4.5±0.1	5±1	20.70	195.4
NHSGS	100	–	–	–	9.4±0.1	10±6	14.09	119.7

Table 2. Midpoint environmental impacts (ReCiPe 2016, H) associated with the laboratory scale production of 1 kg of TiO_2 nanoparticles by SCS, HSGS, and NHSGS, as modelled with the complete inventories reported in Tables S18–S20.

Impact category	Unit	Synthetic procedure		
		SCS	HSGS	NHSGS
global warming	10^3 $kg_{CO_2\ equiv.}$	2.00	3.22	13.4
stratospheric ozone depletion	10^{-4} $kg_{CFC11\ equiv.}$	4.98	4.31	15.7
ionizing radiation	$kBq_{Co\text{-}60\ equiv.}$	14.3	23.5	54.3
ozone formation, human health	$kg_{NOx\ equiv.}$	4.28	7.25	29.3
fine particulate matter formation	$kg_{PM2.5\ equiv.}$	3.80	7.02	28.3
ozone formation, terrestrial ecosystems	$kg_{NOx\ equiv.}$	4.64	7.68	31.3
terrestrial acidification	$kg_{SO_2\ equiv.}$	12.0	22.1	92.7
freshwater eutrophication	$kg_{P\ equiv.}$	0.331	0.505	1.28
marine eutrophication	10^{-2} $kg_{N\ equiv.}$	3.50	5.12	12.0
terrestrial ecotoxicity	10^3 $kg_{1,4\text{-}DCB}$	5.72	14.3	27.9
freshwater ecotoxicity	$kg_{1,4\text{-}DCB}$	48.9	111	255
marine ecotoxicity	$kg_{1,4\text{-}DCB}$	64.5	147	333
human carcinogenic toxicity	$kg_{1,4\text{-}DCB}$	106	283	549
human non-carcinogenic toxicity	10^2 $kg_{1,4\text{-}DCB}$	9.57	21.7	47.1
land use	$m^2a_{crop\ equiv.}$	14.1	23.2	50.8
mineral resource scarcity	$kg_{Cu\ equiv.}$	8.51	16.7	29.5
fossil resource scarcity	10^2 $kg_{oil\ equiv.}$	6.36	9.87	42.0
water consumption	m^3	5.39	7.60	21.0

Table 3. Midpoint environmental impacts (ReCiPe 2016, H) associated with the laboratory scale production of 1000 m^2 of TiO_2 nanoparticles by SCS, HSGS and NHSGS, as modelled with the complete inventories reported in Tables S18–S20.

Impact category	Unit	Synthetic procedure		
		SCS	HSGS	NHSGS
global warming	$kg_{CO_2\ equiv.}$	15.3	16.5	112
stratospheric ozone depletion	10^{-6} $kg_{CFC11\ equiv.}$	3.81	2.21	13.1
ionizing radiation	$kBq_{Co\text{-}60\ equiv.}$	0.110	0.121	0.453
ozone formation, human health	10^{-2} $kg_{NOx\ equiv.}$	3.28	3.71	24.5
fine particulate matter formation	10^{-2} $kg_{PM2.5\ equiv.}$	2.91	3.59	23.6
ozone formation, terrestrial ecosystems	10^{-2} $kg_{NOx\ equiv.}$	3.56	3.93	26.1
terrestrial acidification	10^{-2} $kg_{SO_2\ equiv.}$	9.21	11.3	77.4
freshwater eutrophication	10^{-3} $kg_{P\ equiv.}$	2.53	2.59	10.7
marine eutrophication	10^{-4} $kg_{N\ equiv.}$	2.68	2.62	10.1
terrestrial ecotoxicity	$kg_{1,4\text{-}DCB}$	43.8	73.3	233
freshwater ecotoxicity	$kg_{1,4\text{-}DCB}$	0.374	0.570	2.13
marine ecotoxicity	$kg_{1,4\text{-}DCB}$	0.494	0.755	2.78
human carcinogenic toxicity	$kg_{1,4\text{-}DCB}$	0.809	1.45	4.58
human non-carcinogenic toxicity	$kg_{1,4\text{-}DCB}$	7.33	11.1	39.3
land use	$m^2a_{crop\ equiv.}$	0.108	0.119	0.425
mineral resource scarcity	10^{-2} $kg_{Cu\ equiv.}$	6.52	8.55	24.7
fossil resource scarcity	$kg_{oil\ equiv.}$	4.87	5.05	35.1
water consumption	10^{-2} m^3	4.12	3.89	17.6

Particularly, the impact of SCS to this category results 4.98×10^{-4} $kg_{CFC\text{-}11equiv.}$ (Table 2) and it is due (for 92.73%) to dinitrogen monoxide released into air mainly (for 50.12%) as a consequence of the production of nitric acid (i.e., to the process "Nitric acid, without water, in 50% solution state {RoW}|nitric acid production, product in 50% solution state|APOS, U"), necessary for the nitration reaction.

The large differences in most of the impact categories considered are related to the significantly different amounts of energy necessary for the three synthetic strategies assessed, as a consequence of their different reaction times (as detailed in the Experimental Section and in the inventories reported in Tables S18–S20).

Particularly, the higher percentage of difference between SCS and NHSGS for 1 kg functional unit (-87% for SCS) is found for the terrestrial acidification (TA) impact category. The contributions to this impact category are mainly due to the electric energy needed for the heating plate operation (58.5% for SCS and 69.2% for NHSGS). In both cases, the impact is due for 89.4% to SO_2 released in air, mainly (52.5%) associated to the process "Electricity, bituminous coal, at power plant/US System – Copied from USLCI" comprised in the US electricity mix employed (Table S16).

Similarly, the fine particulate matter formation (FPMF) impact category values for SCS and HSGS are respectively the 13.4% and the 24.8% of the corresponding FPMF value for NHSGS. The contributions to this impact category are again mainly due to the electric energy needed for the heating plate operation (54.1% for SCS, 35.5% for HSGS and 66.2% for NHSGS). Independent of the synthetic strategy, the impact is due for 88.7% to SO_2 released in air, mainly (52.5%) associated to the process "Electricity, bituminous coal, at power plant/US

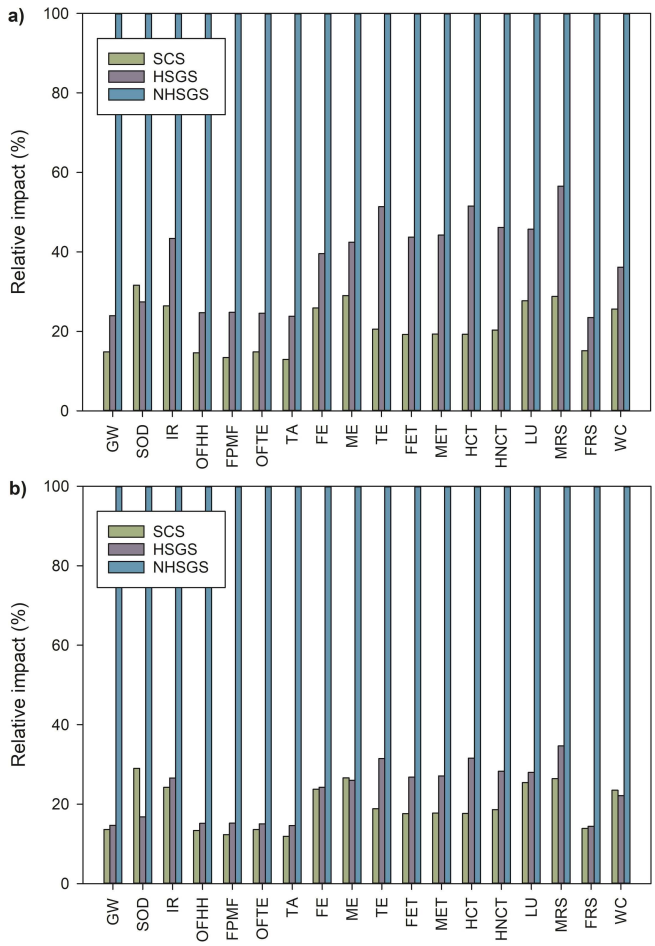

Figure 1. Relative environmental impacts, calculated at a midpoint level (ReCiPe 2016, H), associated with the laboratory scale production of 1 kg (a) and 1000 m^2 surface area (b) of TiO_2 nanoparticles by SCS, HSGS, and NHSGS, as modelled with the complete inventories reported in Tables S18–S20. The impact categories considered by the impact assessment method are: global warming (GW, $kg_{CO_2\ equiv.}$), stratospheric ozone depletion (SOD, $kg_{CFC\text{-}11\,equiv.}$), ionizing radiation (IR, $kBq_{Co\text{-}60\,equiv.}$), ozone formation-human health (OFHH, $kg_{NOx\,equiv.}$), fine particulate matter formation (FPMF, $kg_{PM2.5\,equiv.}$), ozone formation-terrestrial ecosystems (OFTE, $kg_{NOx\,equiv.}$), terrestrial acidification (TA, $kg_{SO_2\ equiv.}$), freshwater eutrophication (FE, $kg_{P\,equiv.}$), marine eutrophication (ME, $kg_{N\,equiv.}$), terrestrial ecotoxicity (TE, $kg_{1,4\text{-}DCB}$), freshwater ecotoxicity (FET, $kg_{1,4\text{-}DCB}$), marine ecotoxicity (MET, $kg_{1,4\text{-}DCB}$), human carcinogenic toxicity (HCT, $kg_{1,4\text{-}DCB}$), human non-carcinogenic toxicity (HNCT, $kg_{1,4\text{-}DCB}$), land use (LU, $m^2a_{crop\,equiv.}$), mineral resource scarcity (MRS, $kg_{Cu\,equiv.}$), fossil resource scarcity (FRS, $kg_{oil\,equiv.}$), and water consumption (WC, m^3).

System—copied from USLCI" comprised in the US electricity mix employed (Table S16).

Slightly different is the situation for the ionizing radiation (IR) impact category. Its values for SCS and HSGS are respectively the 26.4% and the 43.4% of the value for NHSGS. In the case of SCS, the contribution to this impact category is mainly (26.8%) due to the acetone employed for washing the glassware. Particularly, its impact is mainly due (90.8%) to emissions of radon-222 in air, associated principally to the process "Tailing, from uranium milling {GLO}|treatment of|APOS, U". The latter process is related to the mix of electric energy necessary for the wastewater treatment, comprised in the Ecoinvent process "Isopropanol {RoW}|production|APOS, U", needed for the synthesis of acetone. The contributions to IR for HSGS and NHSGS are instead mainly due to the process used to model the activated carbon air filter (for 42.7% and 31.9% respectively). In both cases, the impact is due for 92.1% to radon-222 released in air, mainly (97.2%) associated to the process "Tailing, from uranium milling {GLO}|treatment of|APOS, U". The latter is in this case mainly related to the electricity mix considered in the Ecoinvent process "Activated carbon, granular {RoW}|activated carbon production, granular from hard coal|APOS, U".

In marine eutrophication (ME), the values for SCS and HSGS are the 29% and the 42.5% of the corresponding value for NHSGS. In the case of SCS, the contribution to ME is mainly (23.8%) due to the treatment of the water used for the ice bath, and its impact is due for 55.4% to nitrate released in water, associated for 99.6% to the process "Wastewater, from residence {RoW}|treatment of, capacity 1.1×10^{10} $L\,y^{-1}$|APOS, U" (Table S18). The contributions to ME for HSGS and NHSGS are instead mainly due to the process used to model the cotton lab-coat production (for 37.2% and 27.2% respectively). In both cases, the impact is due for 79.7% to nitrate released in water, mainly (66.9%) associated to the process "Seed-cotton {RoW}|seed-cotton production, conventional|APOS, U".

When considering 1000 m^2 functional unit (Figure 1b), SCS has greater environmental impact than HSGS in two additional categories (i.e., marine eutrophication, ME, $kg_{N\,equiv.}$ and water consumption, WC, m^3). The production of an amount of TiO_2 nanoparticles by SCS corresponding to 1000 m^2 (i.e., ca. 7.66 g) leads to an impact of 2.68×10^{-4} $kg_{N\,equiv.}$ in the ME impact category. This latter contribution is due for 64.15% to the release of nitrate in water, the latter associated for 28.67% to the process "Spoil from hard coal mining {GLO}|treatment of, in surface landfill|APOS, U", describing the landfill disposal of lignite spoils, and mainly (for 51.74%) comprised in the process used to model the activated carbon air filter (Table S15).

The contribution of 1000 m^2 surface area of TiO_2 nanoparticles to WC impact category is 4.12×10^{-2} m^3 (Table 3), and it is due to the consumption of water (i.e., water, turbine use, unspecified natural origin, RoW) associated to the US electricity mix (Table S16) used mainly (for 69.21%) in the evaporating of the reaction mixture to 90 °C and its ignition at 180 °C.

By grouping the results of the eighteen impact categories into the opportune damage categories and referring them at the point at which the environmental effects potentially occur, the endpoint results are obtained as depicted in Figure 2 and quantitatively detailed in Tables S24 and S25 for 1 kg and 1000 m^2 functional units, respectively.

By considering the mass-based functional unit, SCS possesses the lowest environmental impacts within the three damage categories considered, i.e., Human health, Ecosystems and Resources (Figure 2a). When instead the surface area-based functional unit is considered, the impact of SCS in the damage category Resources becomes higher with respect to the one of HSGS (Figure 2b). In details it is equal to 1.25 USD2013 (Table S25) and it is mainly (for 56.95%) due to the consumption of 2.36 m^3 of natural gas considered (for 72.60%) in the USLCI database process named "Natural gas, at extraction site/

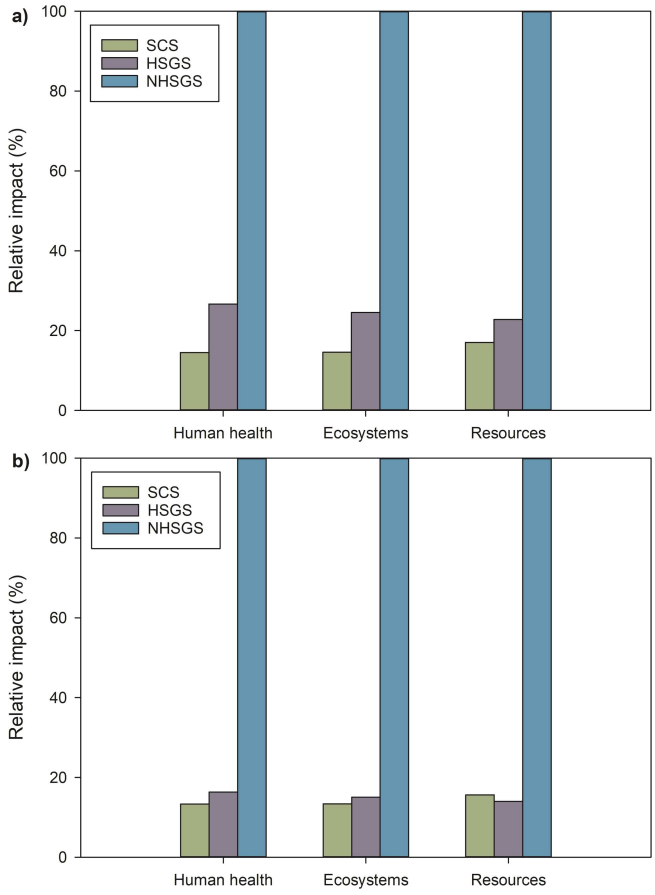

Figure 2. Relative impact [%] associated to the production of 1 kg (a) and 1000 m^2 surface area (b) of TiO_2 nanoparticles synthesised by SCS, HSGS and NHSGS (as modelled with the complete inventories reported in Tables S18–S20) and calculated at the endpoint level, i.e., in terms of the damage categories Human health (DALY), Ecosystems (species year) and Resources (USD2013).

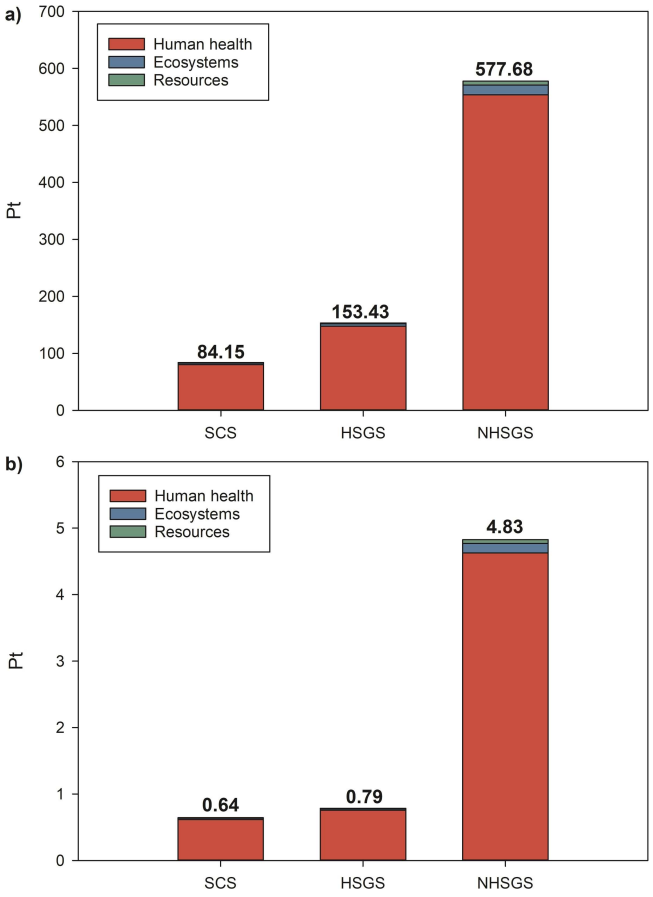

Figure 3. Single score results for the lab-scale production of 1 kg (a) and 1000 m^2 surface area (b) of TiO_2 nanoparticles synthesised by SCS, HSGS and NHSGS (as modelled with the complete inventories reported in Tables S18–S20).

US". This process is comprised in the US electricity mix (Table S16) and its impact is mainly (for 53.69%) due to the electricity needed for the use of the magnetic stirrer heater plate, and secondly (for 17.00%) to the electric energy required by the aspiration system.

To better compare the lab-scale productions of TiO_2 nanoparticles by SCS, HSGS and NHSGS, their environmental loads can be expressed as a single score (i.e., in terms of the eco-indicator point, Pt: the bigger its value is, the higher the impact of that particular process on the environment is), as calculated after normalization and weighting operations. The single score results are depicted in Figure 3 and detailed in Tables 4 and 5, for 1 kg and 1000 m^2 functional units, respectively.

From Figure 3 it is clearly inferable that SCS can effectively be considered a more environmentally sustainable synthetic protocol, with respect to both HSGS and NHSGS. Indeed, independent of the functional unit considered SCS is characterized by the lowest single scores, i.e., 84.15 Pt (considering the mass-based functional unit, Figure 3a) and 0.64 Pt (considering the surface area-based functional unit, Figure 3b). Oppositely, the NHSGS performed in benzyl alcohol represents the most environmentally impacting route, with a total impact of 577.68 Pt when considering 1 kg of TiO_2 nanoparticles, and

Table 4. Detailed single score results for the lab-scale production of 1 kg of TiO_2 nanoparticles synthesised by SCS, HSGS and NHSGS (as modelled with the complete inventories reported in Tables S18–S20).

Damage category	Unit	Synthetic procedure		
		SCS	HSGS	NHSGS
human health	Pt	80.48	147.66	553.71
ecosystems	Pt	2.50	4.21	17.14
resources	Pt	1.16	1.56	6.83
total	Pt	84.15	153.43	577.68

Table 5. Detailed single score results for the lab-scale production of the amounts of TiO_2 nanoparticles corresponding to 1000 m^2 of surface area, synthesised by SCS, HSGS and NHSGS (as modelled with the complete inventories reported in Tables S18–S20).

Damage category	Unit	Synthetic procedure		
		SCS	HSGS	NHSGS
human health	Pt	0.62	0.76	4.63
ecosystems	Pt	0.02	0.02	0.14
resources	Pt	0.01	0.01	0.06
total	Pt	0.64	0.79	4.83

4.83 Pt when considering the amount of powders corresponding to 1000 m^2 of surface area.

To highlight the role of the different sub-processes into the total impact, the single score results, referred to 1 kg functional unit, are detailed for each synthetic protocol in Tables S26–S28 and graphically reported in Figures S10–S12.

The results in Table S26 and Figure S10 highlight that the major contributions to the lab-scale production of 1 kg of TiO_2 nanoparticles by SCS are due to the electric energy necessary for the operation of the heating plate (45.22%) and the aspiration system (14.32%), to the construction of the aspiration system (10.71%) and the activated carbon air filter (9.27%), and to the acetone employed for washing the glassware (7.78%).

Similarly, the main contributions to the impact of HSGS and NHSGS are related to the operation of the heating plate (30.09% and 60.05% respectively) and the aspiration system (25.22% and 11.53% respectively), and to the construction of the aspiration system (18.87% and 8.63% respectively) and the activated carbon filter (16.33% and 7.47% respectively) plants (see Tables S27, S28 and Figures S11, S12).

Necessarily, the three synthesis methods assessed in this work are quite specific and not necessarily optimized from an environmental perspective, but rather in terms of the yield and quality of the target nanoparticles. This means that any potential change performed on the experimental conditions of each strategy, will affect not only the amount and quality of the synthesised TiO_2 nanoparticles, but also the environmental impacts associated to each synthesis.

Therefore, in order to allow the readers and further researchers in the field to re-calculate (at the endpoint level with ReCiPe 2016 H/A impact assessment method) the environmental impacts associated to SCS, HSGS and NHSGS eventually performed with some experimental modifications (e.g., amount of reagents, solvent, energy, etc.) with respect to the procedures here described, the authors developed a simple tool, named "LCIA tool for TiO_2 NPs synthesis by SCS, HSGS and NHSGS", available in Supporting Information. This tool simply consists in three different Excel worksheets (one for each synthesis method assessed) in which it is possible to modify the amounts of the input and output variables as well as the yield and the quality (i.e., crystallinity and humidity degrees) of the obtained TiO_2 nanoparticles. The tool will report both numerically and graphically the new environmental impacts (reported as single scores, Pt) associated to the modified procedures. Hopefully this tool will contribute to further optimizations of the SCS, HSGS and NHSGS, not only on the basis of the amount and quality of the obtained product, but also concurrently accounting for their environmental performances, in order to pursue an always more environmentally sustainable synthesis of TiO_2 nanoparticles.

Sensitivity analysis: the role of electric energy country mix

Since the major contributions to the environmental impacts of the three synthetic strategies assessed in this work are related to the electric energy consumption, a sensitivity analysis was performed to see how the LCA results may vary by employing different electric energy country mixes.

Particularly, the process modelled for the synthesis of titanium (IV) isopropoxide precursor (inventory of Table S17) as well as those related to the synthesis of TiO_2 NPs by SCS, HSGS and NHSGS (inventories of Tables S18–S20) were modified by replacing the electricity mix of Table S16, with those of the six regional entities of the North American Electric Reliability Corporation, NERC (i.e., Western Electricity Coordinating Council WECC, Midwest Reliability Organization MRO, Texas Reliability Entity TRE, Northeast Power Coordinating Council NPCC, ReliabilityFirst Corporation RFC, and South-eastern Electric Reliability Council SERC), the Italian (IT) as well as the State Grid Corporation of China (SGCC) ones.

The single score results (ReCiPe 2016 H/A) of the sensitivity analysis are summarised in Figure 4 and detailed (together with the description of the Ecoinvent datasets used) in Tables S29–S31 for 1 kg of TiO_2 NPs obtained by SCS, HSGS and NHSGS, respectively. Independent of the electric energy mix considered, being equal the latter, the general trend of the environmental impacts (i.e., SCS < HSGS < NHSGS) is still satisfied. The NPCC electricity grid results the one leading to the higher reduction of the environmental impact (from −43.6% for HSGS to −55.2% for NHSGS).

On the opposite, the use of the MRO electricity grid leads to the most significant increase of the environmental impact independent of the synthesis method considered (from +60.0% for SCS to +76.0% for NHSGS).

The observed differences are mainly due to the different mixes characterizing the electricity available on the high voltage level in these regional entities. Particularly the NPCC grid results mainly generated (according to the Ecoinvent dataset "Electricity, high voltage {NPCC, US only}|market for|APOS, U") by nuclear energy (ca. 30%) and by natural gas (ca. 30%).[57,58] Differently, the MRO grid is generated (according to the Ecoinvent dataset "Electricity, high voltage {MRO, US only}|market for|APOS, U") principally by wind power plants (ca.

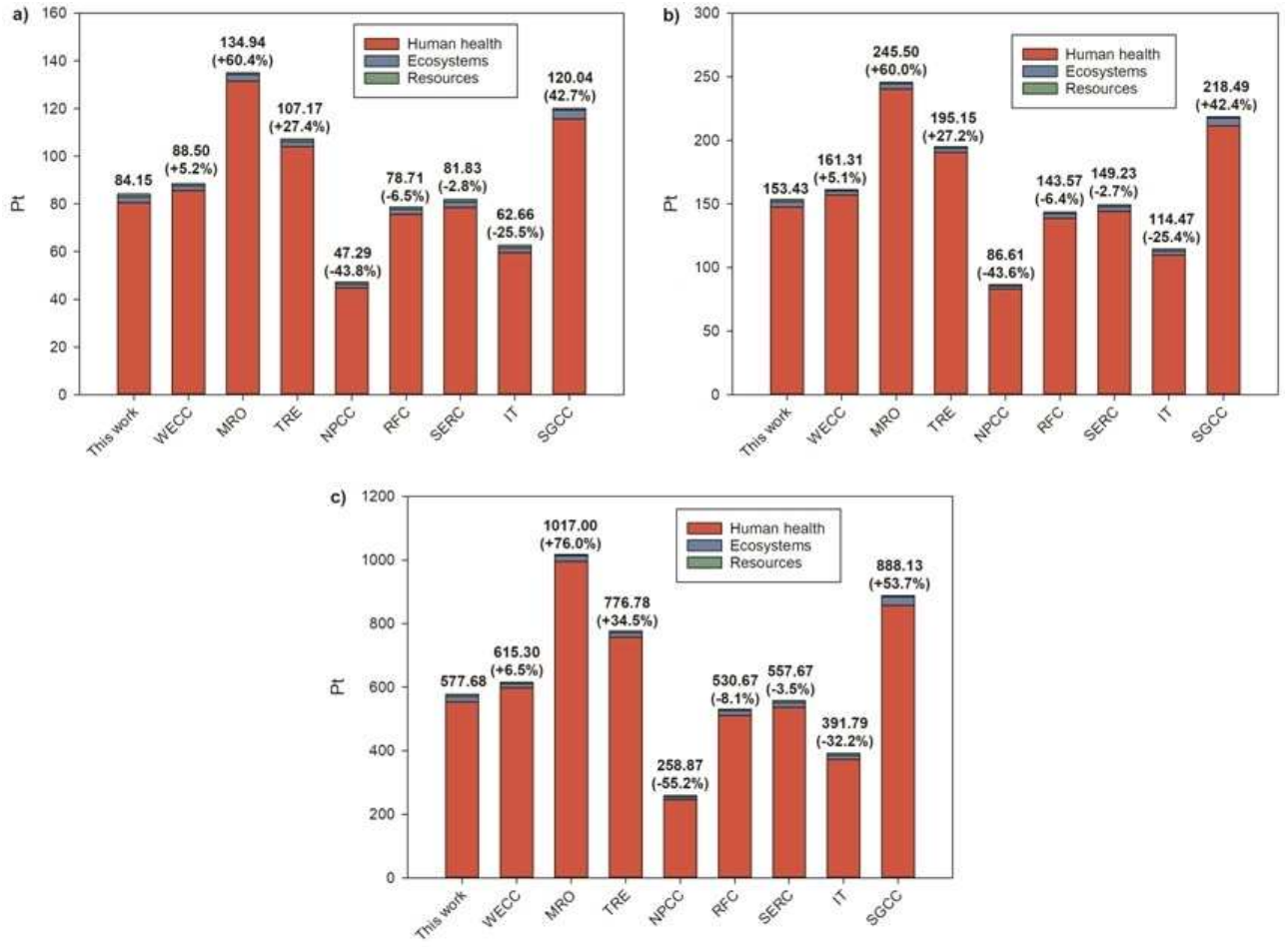

Figure 4. Single score results (ReCiPe 2016 H/A) of the sensitivity analysis for the preparation of 1 kg of TiO_2 nanoparticles by SCS (a), HSGS (b) and NHSGS (c), replacing the electricity mix of this work (i.e., the one reported in Table S16) with those of the six regional entities of the North American Electric Reliability Corporation, NERC (i.e., Western Electricity Coordinating Council WECC, Midwest Reliability Organization MRO, Texas Reliability Entity TRE, Northeast Power Coordinating Council NPCC, ReliabilityFirst Corporation RFC, and South-eastern Electric Reliability Council SERC), the Italian (IT) as well as the State Grid Corporation of China (SGCC) ones.

26%), by burning of lignite (ca. 22%) and by natural gas (ca. 20%).[57,58]

The Italian country energy mix, i.e., the one effectively employed for conducting the synthesis experiments represents a trade-off scenario, since its use leads to reductions of 25.5%, 25.4% and 32.2% to the environmental impacts of SCS, HSGS and NHSGS respectively (Figure 4). At the high voltage level it results (according to the Ecoinvent dataset "Electricity, high voltage {IT}|market for|APOS, U") mainly derived by natural gas (ca. 37%), by hydroelectric power plants (ca. 17%) and by hard coal (ca. 10%).[57,59]

Environmental impact comparison with further chemical, physical and biological synthetic routes

Although the results of Tables S26–S28 and Figures S10–S12 demonstrated the not negligible contribution of the environmental impacts associated to equipment, work-up procedures and reaction-waste treatments, to compare SCS, HSGS and NHSGS to the seven TiO_2 synthetic routes assessed by Wu et al.,[33] their inventories were modified (Tables S21-S23). Particularly, these changes involved the energy contributions that were calculated by Equations (4) and (5), and the contributions of transport, equipment, emissions, and waste treatments that were neglected.

These changes led to a decrease of the impacts of more than 90% (according to ReCiPe 2016 H/A and considering 1 kg functional unit) independent of the synthesis considered (Figure S13). Moreover, the new trend followed by the environmental impacts of the three synthetic strategies is slightly modified in HSGS < SCS < NHSGS (by considering 1 kg functional unit).

The results of the ten synthesis methods compared are visually reported in terms of relative impacts in Figure 5 and accurately detailed in Table 6 (for 1 kg) and Table 7 (for 1000 m^2).

By considering first the mass-based functional unit (i.e., Figure 5a and Table 6), the HSGS assessed in the present study represents the less environmentally impacting synthetic meth-

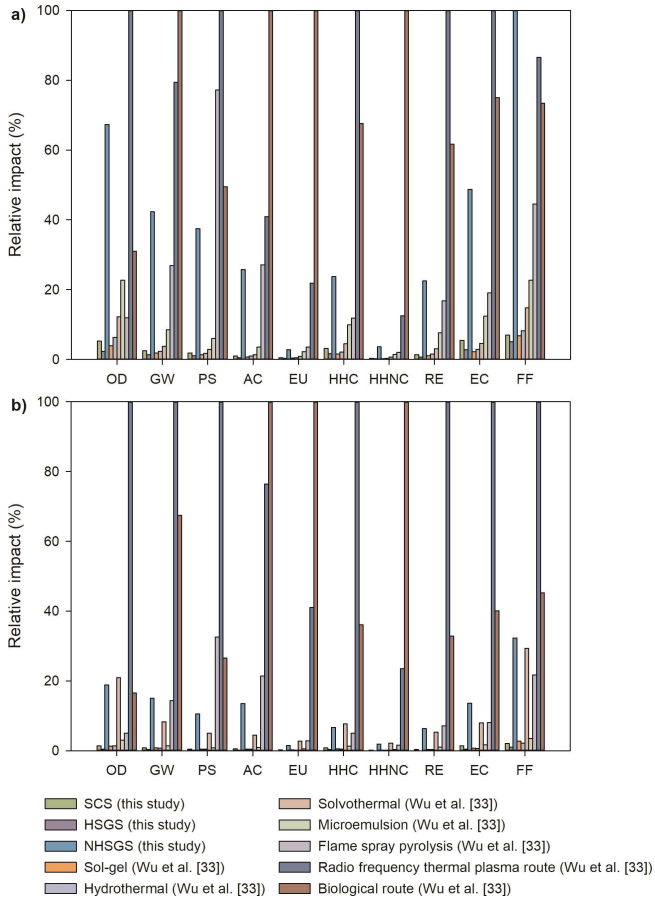

Figure 5. Relative environmental impacts of the ten synthesis methods (i.e., the three of the present study and the seven of the systematic study performed by Wu et al.[33]), as calculated by TRACI 2.1 method, considering the mass-based (a) and the surface area-based (b) functional units. The ten impact categories considered are ozone depletion (OD, $kg_{CFC\text{-}11\ equiv.}$), global warming (GW, $kg_{CO_2\ equiv.}$), smog (PS, $kg_{O_3\ equiv.}$), acidification (AC, $kg_{SO_2\ equiv.}$), eutrophication (EU, $kg_{N\ equiv.}$), carcinogenics (HHC, CTUh: i.e., Comparative Toxic Unit for human toxicity impact), non carcinogenics (HHNC, CTUh), respiratory effects (RE, $kg_{PM2.5\ equiv.}$), ecotoxicity (EC, CTUe: i.e., Comparative Toxic Unit for ecotoxicity), and fossil fuel depletion (FF, $MJ_{surplus}$).

od for all the impact categories considered, except for carcinogenics (HHC) and ecotoxicity (EC), for which instead its impact results higher only with respect to the sol–gel synthesis assessed by Wu et al.[33]

SCS is the third less impacting synthesis in the impact categories ozone depletion (OD), eutrophication (EU), respiratory effects (RE) and fossil fuel depletion (FF), while for the other categories it gets position fourth, with the exception of ecotoxicity (EC) category, for which SCS is at the fifth place.

Oppositely to the good performances of HSGS and SCS, NHSGS in benzyl alcohol occupies always one of the first four positions among the most impacting methods, with the first position occupied in the fossil fuel depletion category and the second one for the ozone depletion.

When re-scaling the environmental impacts based on the surface area of the obtained nanoparticles (Figure 5b and Table 7), the situation improves further for HSGS and SCS. The production of 1000 m^2 of TiO_2 nanoparticles by HSGS possesses the lowest environmental impact among the ten synthesis methods, independent of the impact category. SCS lies always among the four less impacting synthetic strategies, occupying the second position in the fossil fuel depletion impact category and the third one in the categories ozone depletion, smog, eutrophication and respiratory effects. Some environmental improvements are also reached by NHSGS. It never occupies the worst two positions while it lies at the third place or at the fourth one among the most impacting strategies in most of the impact categories considered, with the exception of eutrophication one with respect to which it gets the fifth position.

Independent of the functional unit considered, it can be concluded that also this latter comparison with further chemical, physical and biological synthetic strategies, highlighted the good environmental performances of both HSGS and SCS as assessed in the present study. Although, HSGS represents the less environmentally impacting synthesis method, it should be reminded that these results were obtained by neglecting significant contributions to the life cycles of the ten syntheses assessed (e.g., transport, direct emissions, equipment employed and reaction waste treatments), as a consequence of the lack of primary data employed in the systematic study by Wu et al.,[33] since the latter considered published procedures without replicating the experiments. This means, that the final environmental sustainability ranking obtained, could be potentially upset.

However, by bearing in mind the previously obtained results concerning the comparison between SCS, HSGS and NHSGS as modelled with their complete inventories, in which SCS demonstrated a lower environmental impact with respect to other methods, it can be argued that SCS can be considered an environmentally sustainable synthetic strategy for the obtainment of TiO_2 nanoparticles.

Conclusions

Solution combustion synthesis (SCS) of TiO_2 nanoparticles has been for the first time assessed from an environmental perspective and compared with hydrolytic sol–gel synthesis (HSGS) and non-hydrolytic sol–gel synthesis (NHSGS), by the life cycle assessment (LCA) methodology.

The possibility to experimentally replicate the procedures described into the literature allowed to model the inventories of the studied systems in a more detailed and trustworthy way, thus accounting also for information that are typically neglected (e.g., amount of solvents used for the work-up and waste generated), while instead constituting fundamental inputs to build up the life cycle stages of a given synthetic protocol performed at a lab scale.

Independent of the functional unit considered, i.e., 1 kg of nanoparticles or 1000 m^2 of surface area, the SCS, assessed in this study, demonstrated to be more environmentally sustainable with respect to sol–gel strategies performed both in water and in benzyl alcohol, at least in the specific experimental conditions considered in this study. Particularly, its environmental impact resulted 45.15% and 85.43% lower with respect

Table 6. Detailed midpoint environmental impacts (TRACI 2.1 method) associated with the laboratory scale production of 1 kg of TiO_2 nanoparticles by SCS, HSGS, NHSGS (as modelled with the inventories reported in Tables S21–S23), and the seven synthetic routes assessed in the systematic study by Wu et al.[33]

Impact category	Unit	Synthetic procedure			sol–gel[33]	hydrothermal[33]	solvothermal[33]	microemulsion[33]	flame spray pyrolysis[33]	radio frequency thermal plasma route[33]	biological[33]
		SCS	HSGS	NHSGS							
OD	10^{-6} $kg_{CFC\text{-}11\ equiv.}$	4.52	2.01	57.3	3.32	5.38	10.4	19.3	10.2	85.1	26.4
GW	10^{2} $kg_{CO_2\ equiv.}$	0.659	0.349	11.1	0.484	0.609	0.993	2.22	7.04	20.8	26.2
PS	$kg_{O_3\ equiv.}$	3.17	1.78	64.1	2.39	3.06	4.94	10.3	132	171	84.7
AC	$kg_{SO_2\ equiv.}$	0.337	0.168	8.54	0.243	0.320	0.454	1.18	9.01	13.6	33.2
EU	$kg_{N\ equiv.}$	0.125	0.0755	0.742	0.101	0.128	0.230	0.614	0.967	5.89	26.9
HHC	10^{-6} CTUh	2.55	1.36	19.1	1.27	1.70	3.60	7.97	9.56	80.6	54.5
HHNC	10^{-6} CTUh	8.81	4.75	88.2	6.02	8.39	16.1	35.9	50.0	308	$2.45{\cdot}10^{3}$
RE	10^{-2} $kg_{PM2.5\ equiv.}$	3.31	1.71	52.9	2.56	3.64	7.24	17.9	39.5	235	145
EC	10^{2} CTUe	5.78	2.97	51.6	2.34	3.07	4.92	13.2	20.2	106	79.5
FF	10^{2} $MJ_{surplus}$	1.48	1.08	21.2	1.45	1.75	3.14	4.82	9.47	18.4	15.6

to HSGS and NHSGS respectively, when considering the mass based functional unit. The use of 1000 m^2 surface area as the functional unit for the comparison, increased the environmental gap with respect to NHSGS (up to −86.75% of difference) and reduced the one from HSGS (down to −18.99% of difference).

The sensitivity analysis performed to investigate the role of the electricity country mix considered, did not alter the general trend observed for the environmental impacts associated to the syntheses of 1 kg of TiO_2 nanoparticles (i.e., SCS < HSGS < NHSGS). However, significant differences were highlighted, with the NPCC (i.e., the U.S. Northeast Power Coordinating Council) grid that resulted the one potentially leading to the higher reduction of the environmental impacts, among those investigated.

The environmental impacts of these three different syntheses were also reliably compared with those associated with seven further strategies recently assessed in a systematic study, i.e., sol–gel, hydrothermal, solvothermal, microemulsion, flame spray pyrolysis, radio frequency thermal plasma and biological synthesis. In doing so significant contributions to the whole impacts needed necessarily to be neglected. This latter comparison highlighted the highest environmental performances of the HSGS as modelled in the present study, with SCS laying however among the less environmentally impacting procedures. On the contrary, NHSGS performed by following the benzyl alcohol route positioned itself among the most impacting ones like the radio frequency thermal plasma and the biological synthetic route, especially when considering the mass-based functional unit.

Based on the two comparison studies, SCS can be considered a more environmentally sustainable procedure, at least for the synthesis of TiO_2 nanoparticles, now with quantitative environmental impact data at support of this statement. However, to obtain trustworthy environmental impact assessments, it should be highlighted the need to comprise also the contributions of transport, equipment, work-up procedures, waste treatment and emissions. At this latter regard, replication of the published synthetic procedures is highly recommended, even because the experimental results can slightly differ from the published ones, thus potentially affecting the results of the environmental assessment performed by LCA methodology.

The here presented results refer to lab-scale procedures that typically are not optimized, therefore they do not necessarily reflect the results of upscaled industrial syntheses (usually characterized by significant reductions of materials and energy consumptions), which instead would need to be considered on a case-to-case basis.

Therefore, it is highly desirable that future LCA research studies will be always more frequently accompanied by simple tools as the "LCIA tool for TiO_2 NPs synthesis by SCS, HSGS and NHSGS" presented in this work since it would allow to partially overcome the process specificity related limitations of the presented results, concurrently contributing to the optimization of a given process/product (also at a lab-scale) by considering in real time its environmental impacts, without having to perform a new LCA study.

Table 7. Detailed midpoint environmental impacts (TRACI 2.1 method) associated with the laboratory scale production of 1000 m^2 surface area of TiO_2 nanoparticles by SCS, HSGS, NHSGS (as modelled with the inventories reported in Tables S21–S23), and the seven synthetic routes assessed in the systematic study by Wu et al.[33]

Impact category	Unit	Synthetic procedure									
		SCS	HSGS	NHSGS	sol–gel[33]	hydrothermal[33]	solvothermal[33]	microemulsion[33]	flame spray pyrolysis[33]	radio frequency thermal plasma route[33]	biological[33]
OD	10^{-8} $kg_{CFC\text{-}11\ equiv.}$	3.46	1.03	47.8	3.33	3.59	53.1	7.53	12.8	254	42.0
GW	$kg_{CO_2\ equiv.}$	0.504	0.179	9.26	0.491	0.412	5.11	0.871	8.84	61.9	41.7
PS	10^{-2} $kg_{O_3\ equiv.}$	2.42	0.910	53.5	2.43	2.07	25.4	4.02	166	510	135
AC	10^{-3} $kg_{SO_2\ equiv.}$	2.58	0.857	71.4	2.49	2.18	23.5	4.62	113	404	529
EU	10^{-3} $kg_{N\ equiv.}$	0.959	0.386	6.20	1.01	0.853	11.8	2.40	12.2	176	429
HHC	10^{-8} CTUh	1.95	0.695	16.0	1.27	1.14	18.4	3.11	12.0	240	86.7
HHNC	10^{-7} CTUh	0.675	0.243	7.36	0.607	0.562	8.28	1.40	6.28	91.9	391
RE	10^{-4} $kg_{PM2.5\ equiv.}$	2.53	0.877	44.2	2.59	2.45	37.2	7.00	49.7	701	230
EC	CTUe	4.43	1.52	43.1	2.36	2.06	25.3	5.17	25.4	317	127
FF	$MJ_{surplus}$	1.14	0.553	17.8	1.46	1.17	16.1	1.89	11.9	54.9	24.8

Experimental Section

Materials and methods

Similar to the work by Wu et al.,[33] laboratory scale procedures were assessed in this work due to both the recently recognized importance of framing also lab-scale processes in the context of their life cycles[60–62] and the typical lack of synthesis information at an industrial scale.

The selection of the solution combustion synthesis of TiO_2 nanoparticles and the sol–gel approaches was performed based on some of the criteria considered by Wu et al.,[33] like for example the use of the same precursor and the presence of a full characterization of the obtained product. However, all the synthetic protocols selected were replicated in the laboratory to experimentally determine data typically neglected in the published procedures (e.g., amount of solvent needed for the work-up, etc.), to model them more accurately.

Titanium(IV) isopropoxide (97%), glycine (≥99%), Triton X-100 (laboratory grade), benzyl alcohol (≥99%) and acetic acid (≥99.8%) were purchased from Sigma–Aldrich (Milan, Italy), while HNO_3 (65%) and HCl (37%) from Fischer Scientific (Milan, Italy), petroleum ether (40–60) from Carlo Erba reagents s.r.l (Milan, Italy) and acetone (technical grade) from Incofar s.r.l. (Modena, Italy). They all were used as received, without further purification.

The environmental performances of SCS, HSGS and NHSGS considered in the present study for the preparation of TiO_2 nanoparticles were assessed according to the reaction mechanisms and conditions reported in the following subsections.

Solution combustion synthesis of TiO_2 nanoparticles

SCS of TiO_2 nanoparticles, was performed according to the procedure reported by Lopera et al.,[63] with a few modifications. In a typical experiment, 3 mL of Ti^{IV} isopropoxide were dropwise added to 25 mL of deionized water in a round bottomed flask and the mixture was stirred at 0 °C for 1 h in order to obtain titanyl hydroxide according to Equation (6), as visually indicated by the appearance of a white precipitate.

$$Ti(C_3H_7O)_4 + 3H_2O \rightarrow TiO(OH)_2 + 4C_3H_7OH \quad (6)$$

Subsequently the as prepared solution was added with 4.17 mL of 65% HNO_3 to quantitatively produce titanyl nitrate according to the following Equation (7).

$$TiO(OH)_2 + 2HNO_3 \rightarrow TiO(NO_3)_2 + 2H_2O \quad (7)$$

The as obtained titanyl nitrate (in a solution state) was mixed under stirring with 1.04 g of glycine fuel to form the precursors solution. The latter was transferred to an alumina crucible that was then heated on a hot plate at 90 °C to slowly remove the water, until a viscous white mass was obtained. The hot plate was then set to the temperature of ca. 180 °C in order to ignite the combustion synthesis reaction reported in Equation (8).

$$9TiO(NO_3)_2 + 10C_2H_5NO_2 \rightarrow 9TiO_2 + 14N_2 + 20CO_2 + 25H_2O \quad (8)$$

After reaction completion, the crucible was removed, allowed to cool down to room temperature and 845 mg of foam type powder were recovered.

Hydrolytic sol–gel synthesis of TiO_2 nanoparticles

The present authors already assessed from an environmental perspective a hydrolytic sol–gel synthesis of TiO_2 nanoparticles,[30] i.e., the procedure patented by Colorobbia S.p.A (one of the most important Italian suppliers of chemicals for the building sector).[31] That procedure yielded as product a 6 wt% TiO_2 suspension in water, characterized by TiO_2 nanoparticles of 30 nm in size. In order to account for the optimization steps performed over the recent years by the patent owners as well as the necessary steps to obtain TiO_2 powders rather than a water suspension, the previously studied procedure was slightly updated and performed at a laboratory scale as follow, in order to obtain results more reliably comparable with those of other syntheses.

A three necked round bottomed flask equipped with an additional funnel, a mechanical stirrer and a thermometer, was charged with a solution of Triton X-100 in H_2O/HCl (77 mL). The amounts of reactants in this mixture were adjusted to have 100 ppm of Triton X-100 and 2.38 wt% (0.25 equiv.) of HCl in the final mixture. 23 g of Ti^{IV} isopropoxide were then dropwise added over 5 min while stirring at 400 rpm. At the end of the additions, the temperature of the reaction mixture (white flakes suspension) was of approximately 40 °C. The round bottomed flask was placed in a pre-heated oil bath at 50 °C under continuous stirring. The mixture was left on stirring at 50 °C for an overall reaction time of 24 h, then it was cooled down to room temperature, transferred into an aluminum bowl and then dried in an oven for 4 days at 120 °C. The as obtained white powders (8.182 g) were then carefully grinded and subjected to subsequent characterization.

The stoichiometric reaction describing the overall hydrolytic sol–gel synthesis of TiO_2 nanoparticles can be expressed by Equation (9).

$$Ti(C_3H_7O)_4 + 2H_2O \rightarrow TiO_2 + 4\,C_3H_7OH \quad (9)$$

Non-hydrolytic sol–gel synthesis of TiO_2 nanoparticles via the benzyl alcohol route

For the non-hydrolytic sol–gel synthesis of TiO_2 nanoparticles, the well-known BAR was performed.[64] Particularly a procedure slightly modified from the work by Melcarne et al.[65] was followed.

In a typical experiment, 3 mL of $Ti(O^iPr)_4$ were dropwise added to benzyl alcohol (14.4 mL) at room temperature in a Schlenk tube under stirring, and then 0.6 mL of acetic acid were introduced. The closed Schlenk tube was then introduced in a pre-heated oil bath at 200 °C and the reaction was prolonged under stirring for 24 h, during which a white precipitate was formed. The reaction mixture was then allowed to cool down to room temperature and transferred to a Falcon tube. The Schlenk was rinsed with acetone (18 mL) and the washings merged with the reaction mixture, which was then centrifuged (4000 rpm, 15 min). After removal of the supernatant, the white solid obtained was again suspended in acetone (35 mL), stirred 5 min, and centrifugation was repeated in the same conditions. After removal of the supernatant, the white solid was suspended in petroleum ether (50 mL), stirred 5 min, and centrifugation was repeated again in the same conditions. The solvent was removed and the solid was dried in air and then under vacuum (50 mbar, 3 h) to give the final product in quantitative yield (961 mg).

The stoichiometric reaction describing the overall non-hydrolytic sol–gel synthesis of TiO_2 nanoparticles can be expressed by Equation (10). The reaction is catalytic in acetic acid and has a complex ligand exchange followed by insertion and elimination mechanism, as reported by Zimmermann et al.[66,67]

$$Ti(C_3H_7O)_4 + 4\,C_6H_5CH_2OH \rightarrow TiO_2 + 4\,C_3H_7OH + 2\,C_6H_5CH_2OCH_2C_6H_5 \quad (10)$$

Characterization

The specific surface area (SSA) of the as synthesized nanoparticles was determined using a Gemini 2360 surface area analyzer from Micromeritics (Norcross, GA, 30093, USA). The powders were degassed under N_2 flux at 105 °C for 24 h before measurements, which were performed on dried specimens. The weight difference before and after degassing operation allowed determining the humidity degree of the as synthesized nanoparticles. Gas adsorption data were evaluated by the BET theory.

X-ray powder diffraction (XRPD) data and Rietveld refinements were used to quantify the various phases in the powders (i.e., TiO_2 polymorphs in addition to amorphous material) and to obtain microstructural information in term of crystallite size. Data were collected using a PANAlytical (Enigma Business Park, Grovewood Road WR14 1XZ, United Kingdom) X'Pert PRO diffractometer (Cu–Kα radiation, $\lambda = 1.5405$ Å) equipped with a fast detector (X'Celerator). The incident beam size was restricted by a divergence slit and an anti-scattering slit (both 0.25°) as well as by a beam mask (15 mm). Soller slits (0.04 rad) were mounted both in the incident and the diffracted beam pathways. The diffracted beam also passed a Ni filter and an antiscatter blade (5 mm) before reaching the detector. Data in the 2θ range 10–90° were collected using a virtual step scan of 0.0167°2θ with a counting time of 50 s per step. Powders for XRPD analyses were prepared as follows: the as-synthesized powders were dried under inert gas flux at 105 °C for 24 h and subsequently mixed with a known amount of internal standard (10 wt% NIST SRM 676a, α-Al_2O_3). The resulting powder was subsequently mounted in a glass sample holder by side-loading. The addition of an internal standard allowed to quantitatively determine the amorphous fraction in the as-synthesized and dried powders, as described elsewhere.[68]

Rietveld refinements were accomplished with the GSAS package[69] and its graphical interface EXPGUI.[70] The background was fitted with a Chebyshev function with 9 coefficients. The peak profiles were modelled using a multiterm Simpson's rule integration of the pseudo-Voigt function (denoted as profile function 2 in GSAS). A Lorentzian size broadening term (LX in GSAS) was refined whereas a Lorentzian strain broadening term (LY in GSAS), a Gaussian term (GW in GSAS) as well as peak asymmetry term were fixed to values refined for a line profile standard (NIST RSM 660c, LaB_6). The XRPD data for the standard were collected using the same instrumental set-up as the one used for sample analyses. The lattice constants of the TiO_2 polymorphs, scale factors for all phases and the zero shift were refined. The weight fractions of the crystalline sample phases as well as the standard (i.e., α-Al_2O_3), that were obtained as output from the Rietveld refinements, were subsequently used to determine the actual phase composition of the sample including the amorphous fraction according to previously described procedures.[68] The crystallite size (D) in Å was calculated according to the following Equation (11),[69] where K is the Scherrer constant, λ is the wavelength [Å], and X is the Lorentzian–Scherrer sample broadening.

$$D = \frac{18000K\lambda}{\pi X} \quad (11)$$

This latter parameter was the refined value of LX following subtraction of the instrumental contribution of this profile parameter (represented by the refined value of this coefficient for the line profile standard NIST RSM 660c).

Transmission electron microscopy (TEM) analyses were performed using a Talos F200s G2 instrument (Thermo Fisher Scientific) equipped with a Schottky field emitter (S-FEG). The particles were deposited on the sample holder, a copper grid with carbon film, by immersion in a previously prepared ethanol dispersion of the TiO_2 powders. The grids were dried under ambient conditions before analyses.

Manual image processing was applied on calibrated micrographs using Image J.[71] The size of the particles composing SCS and HSGS powders were rather isotropic. For these samples, the horizontal diameter of the particle was measured. The particles composing the NHSGS powder were elongated wherefore the minimum and maximum dimensions were measured regardless of orientation. Reported values are means and standard deviations of at least 50 particles.

Acknowledgements

The authors acknowledge Ella Maru Studio for the image reported in the Table of Content. Open Access funding provided by Università degli Studi di Modena e Reggio Emilia within the CRUI-CARE Agreement.

Conflict of Interest

The authors declare no conflict of interest.

Data Availability Statement

The data that support the findings of this study are available in the supplementary material of this article.

Keywords: titanium dioxide · environmental impact · sol–gel synthesis · solution combustion synthesis · life cycle assessment

[1] American Chemistry Council, *Consideration for a Definition for Engineered Nanomaterials*, Arlington, Va, USA: The American Chemistry Council – Nanotechnology Panel, **2007**, https://www.americanchemistry.com/.
[2] Y. Wang, N. Herron, *J. Phys. Chem.* **1991**, *95*, 525–532.
[3] C. R. Berry, *Phys. Rev.* **1967**, *161*, 848–851.
[4] P. T. Anastas, J. C. Warner, *Green Chemistry: Theory and Practice*, Oxford University Press, New York, **1998**.
[5] P. T. Anastas, J. B. Zimmerman, *Environ. Sci. Technol.* **2003**, *37*, 94 A-101 A.
[6] T. Van Gerven, A. Stankiewicz, *Ind. Eng. Chem. Res.* **2009**, *48*, 2465–2474.
[7] R. A. Sheldon, *ACS Sustainable Chem. Eng.* **2018**, *6*, 32–48.
[8] J. Andraos, *ACS Sustainable Chem. Eng.* **2016**, *4*, 1917–1933.
[9] A. Anctil, C. W. Babbitt, R. P. Raffaelle, B. J. Landi, *Environ. Sci. Technol.* **2011**, *45*, 2353–2359.
[10] L. Pourzahedi, M. J. Eckelman, *Environ. Sci. Technol.* **2015**, *49*, 361–368.
[11] A. Varma, A. S. Mukasyan, A. S. Rogachev, K. V. Manukyan, *Chem. Rev.* **2016**, *116*, 14493–14586.
[12] K. Rajeshwar, N. R. de Tacconi, *Chem. Soc. Rev.* **2009**, *38*, 1984–1998.
[13] W. Wen, J. M. Wu, *RSC Adv.* **2014**, *4*, 58090–58100.
[14] R. K. Tukhtaev, V. V. Boldyrev, A. I. Gavrilov, S. V. Larionov, L. I. Myachina, Z. A. Savel'eva, *Inorg. Mater.* **2002**, *38*, 985–991.
[15] S. Arora, S. S. Manoharan, *J. Phys. Chem. Solids* **2007**, *68*, 1897–1901.
[16] R. Amutha, M. Muruganandham, G. J. Lee, J. J. Wu, *J. Nanosci. Nanotechnol.* **2011**, *11*, 7940–7944.
[17] G. R. Rao, B. G. Mishra, H. R. Sahu, *Mater. Lett.* **2004**, *58*, 3523–3527.
[18] A. Kumar, E. E. Wolf, A. S. Mukasyan, *AIChE J.* **2011**, *57*, 2207–2214.
[19] A. Kumar, E. E. Wolf, A. S. Mukasyan, *AIChE J.* **2011**, *57*, 3473–3479.
[20] K. V. Manukyan, A. Cross, S. Roslyakov, S. Rouvimov, A. S. Rogachev, E. E. Wolf, A. S. Mukasyan, *J. Phys. Chem. C* **2013**, *117*, 24417–24427.
[21] A. S. Mukasyan, P. Dinka, WO2007019332-A1, **2007**.
[22] A. T. Aruna, A. S. Mukasyan, *Curr. Opin. Solid State Mater. Sci.* **2008**, *12*, 44–50.
[23] F. T. Li, J. Ran, M. Jaroniec, S. Z. Qiao, *Nanoscale* **2015**, *7*, 17590–17610.
[24] S. Hellweg, L. Milà i Canals, *Science* **2014**, *344*, 1109–1113.
[25] D. P. Macwan, P. N. Dave, S. Chaturvedi, *J. Mater. Sci.* **2011**, *46*, 3669–3686.
[26] Y. F. Chen, C. Y. Lee, M. Y. Yeng, H. T. Chiu, *J. Cryst. Growth* **2003**, *274*, 363–370.
[27] G. F. Grubb, B. R. Bakshi, *J. Ind. Ecol.* **2011**, *15*, 81–95.
[28] P. Caramazana-Gonzalez, P. W. Dunne, M. Gimeno-Fabra, M. Zilka, M. Ticha, B. Stieberova, F. Freiberg, J. McKechnie, E. Lester, *Green Chem.* **2017**, *19*, 1536–1547.
[29] M. P. Tsang, G. Philippot, C. Aymonier, G. Sonnemann, *ACS Sustainable Chem. Eng.* **2018**, *6*, 5142–5151.
[30] M. Pini, R. Rosa, P. Neri, F. Bondioli, A. M. Ferrari, *Green Chem.* **2015**, *17*, 518–531.
[31] G. Baldi, M. Bitossi, A. Barzanti, US0317959 A1, **2008**.
[32] D. Verhulst, B. Sabacky, T. Spitler, W. Duyvesteyn, *CIM Bull.* **2002**, *95*, 89–94.
[33] F. Wu, Z. Zhou, A. L. Hicks, *Env. Sci. Technol.* **2019**, *53*, 4078–4087.
[34] S. Liu, M. M. Mohammadi, M. T. Swihart, *Chem. Eng. J.* **2021**, *405*, 126958.
[35] P. Anastas, M. Nolasco, F. Kerton, M. Kirchhoff, P. Licence, T. Pradeep, B. Subramaniam, A. Moores, *ACS Sustainable Chem. Eng.* **2021**, *9*, 8015–8017.
[36] T. Pradeep, Z. Li, R. Luque, *ACS Sustainable Chem. Eng.* **2021**, *9*, 14327–14329.
[37] ISO 14040:2006, Environmental management – Life cycle assessment – Principles and framework, https://www.iso.org/standard/37456.html.
[38] ISO 14044:2006, Environmental management – Life cycle assessment – Requirements and guidelines, https://www.iso.org/standard/38498.html.
[39] A. Rahman, S. Kang, S. McGinnis, P. J. Vikesland, *ACS Sustainable Chem. Eng.* **2022**, *10*, 3155–3165.
[40] T. Ohno, K. Sarukawa, K. Tokieda, M. Matsumura, *J. Catal.* **2001**, *203*, 82–86.
[41] J. Giménez, B. Bayarri, Ó. González, S. Malato, J. Peral, S. Esplugas, *ACS Sustainable Chem. Eng.* **2015**, *3*, 3188–3196.
[42] A. G. Parvatker, M. J. Eckelman, *ACS Sustainable Chem. Eng.* **2019**, *7*, 350–367.
[43] R. L. Smith, G. J. Ruiz-Mercado, D. E. Meyer, M. A. Gonzalez, J. P. Abraham, W. M. Barrett, P. M. Randall, *ACS Sustainable Chem. Eng.* **2017**, *5*, 3786–3794.
[44] R. Rosa, R. Spinelli, P. Neri, M. Pini, S. Barbi, M. Montorsi, L. Maistrello, A. Marseglia, A. Caligiani, A. M. Ferrari, *ACS Sustainable Chem. Eng.* **2020**, *8*, 14752–14764.
[45] M. Pini, S. Scarpellini, R. Rosa, P. Neri, A. F. Gualtieri, A. M. Ferrari, *Environ. Sci. Technol.* **2021**, *55*, 12672–12682.
[46] Regulation (EC) No. 715/2007 of the European Parliament and of the Council, Official Journal of the European Union, L 171/1, June 29, 2007, can be found under https://eur-lex.europa.eu/legal-content/EN/TXT/PDF/?uri=CELEX:32007R0715&from=EN.
[47] B. P. Weidema, C. Bauer, R. Hischier, C. Mutel, T. Nemecek, J. Reinhard, C. O. Vadenbo, G. Wernet, "The Ecoinvent Database: Overview and Methodology, Data Quality Guideline for the Ecoinvent Database Version 3", can be found under http://www.ecoinvent.org (accessed 20 April 2022).
[48] G. Wernet, C. Bauer, B. Steubing, J. Reinhard, E. Moreno-Ruiz, B. Weidema, *Int. J. Life Cycle Assess.* **2016**, *21*, 1218–1230.
[49] "Federal LCA Commons", can be found under http://lcacommons.gov (accessed 24 April 2022).

[50] "Pré Sustainability, Stationsplein 121, 3818 LE Amersfoort, The Netherlands", can be found under https://simapro.com/contact/ (accessed 20 April 2022).
[51] M. A. J. Huijbregts, Z. J. N. Steinmann, P. M. F. Elshout, G. Stam, F. Verones, M. Vieira, M. Zijp, A. Hollander, R. van Zelm, *Int. J. Life Cycle Assess.* **2017**, *22*, 138–147.
[52] M. Iturrondobeitia, C. Vallejo, M. Berroci, O. Akizu-Gardoki, R. Minguez, E. Lizundia, *ACS Sustainable Chem. Eng.* **2022**, *10*, 9798–9810.
[53] D. Kang, M. Choi, D. Kim, J. Han, *ACS Sustainable Chem. Eng.* **2022**, *10*, 5888–5894.
[54] R. Rosa, M. Pini, G. M. Cappucci, A. M. Ferrari, *Curr. Opin. Green Sustain. Chem.* **2022**, *37*, 100654.
[55] "Tool for Reduction and Assessment of Chemicals and Other Environmental Impacts (TRACI)", can be found under https://www.epa.gov/chemical-research/tool-reduction-and-assessment-chemicals-and-other-environmental-impacts-traci (accessed 26 July 2022).
[56] Y. Zheng, B. Nowack, *Environ. Sci. Technol.* **2021**, *55*, 2392–2402.
[57] IEA World Energy Statistics and Balances. OECD iLibrary, eISSN: 1683–4240, can be found under https://doi.org/10.1787/enestats-data-en (accessed 27 December 2022).
[58] US EPA: Emissions and Generation Resource Integrated Database, can be found under https://www.epa.gov/energy/emissions-generation-resource-integrated-database-egrid (accessed 27 December 2022).
[59] ENTSO–E: Physical Energy & Power Flows, can be found under https://www.entsoe.eu/data/power-stats/physical-flows/ (accessed 27 December 2022).
[60] D. T. Allen, B. J. Hwang, P. Licence, T. Pradeep, B. Subramaniam, *ACS Sustainable Chem. Eng.* **2015**, *3*, 2359–2360.
[61] M. Pini, R. Rosa, P. Neri, A. M. Ferrari in *Life Cycle Assessment in the Chemical Product Chain: Challenges, Methodological Approaches and Applications*, (Eds. S. Maranghi, C. Brondi), Springer, Cham, **2020**, pp. 101–123.
[62] B. Subramaniam, P. Licence, A. Moores, D. T. Allen, *ACS Sustainable Chem. Eng.* **2021**, *9*, 3977–3978.
[63] A. A. Lopera, E. A. Chavarriaga, H. A. Estupiñan, I. C. Valencia, C. Paucar, C. P. Garcia, *J. Phys. D* **2016**, *49*, 205501.
[64] M. Niederberger, M. H. Bartl, G. D. Stucky, *Chem. Mater.* **2002**, *14*, 4364–4370.
[65] G. Melcarne, L. De Marco, E. Carlino, F. Martina, M. Manca, R. Cingolani, G. Gigli, G. Ciccarella, *J. Mater. Chem.* **2010**, *20*, 7248–7254.
[66] M. Zimmermann, G. Garnweitner, *Chem. Ing. Tech.* **2014**, *86*, 231–237.
[67] M. Zimmermann, G. Garnweitner, *CrystEngComm* **2012**, *14*, 8562–8568.
[68] A. F. Gualtieri, *J. Appl. Crystallogr.* **2000**, *33*, 267–278.
[69] A. C. Larson, R. B. Von Dreele, General Structure Analysis System (GSAS), Los Alamos National Laboratory Report LAUR 86–748, Los Alamos National Laboratory (USA), **2004**, https://11bm.xray.aps.anl.gov/documents/GSASManual.pdf.
[70] B. H. Toby, *J. Appl. Crystallogr.* **2001**, *34*, 210–213.
[71] T. J. Collins, *BioTechniques* **2007**, *43*, S25–S30.

Manuscript received: November 27, 2022
Revised manuscript received: January 3, 2023
Accepted manuscript online: January 5, 2023
Version of record online: February 27, 2023